The Prognostic Role of *MYC* Structural Variants Identified by NGS and FISH in Multiple Myeloma

Neeraj Sharma[1], James B. Smadbeck[2], Nadine Abdallah[3], Cinthya Zepeda-Mendoza[4], Moritz Binder[3], Kathryn E. Pearce[1], Yan W. Asmann[5], Jess F. Peterson[1,6], Rhett P. Ketterling[1,6], Patricia T. Greipp[1,6], P. Leif Bergsagel[7], S. Vincent Rajkumar[3], Shaji K. Kumar[3], and Linda B. Baughn[1,6]

ABSTRACT

Purpose: Structural variants (SV) of the *MYC* gene region are common in multiple myeloma and influence disease progression. However, the prognostic significance of different *MYC* SVs in multiple myeloma has not been clearly established.

Experimental Design: We conducted a retrospective study of multiple myeloma comparing *MYC* SV subtypes identified by next-generation sequencing (NGS) and FISH to *MYC* expression and disease survival using 140 cases from Mayo Clinic and 658 cases from the MMRF CoMMpass study.

Results: *MYC* SVs were found in 41% of cases and were classified into nine subtypes. A correlation between the presence of a *MYC* SV and increased *MYC* expression was identified. Among the nine *MYC* subtypes, the non-immunoglobulin (non-Ig) insertion sub-

type was independently associated with improved outcomes, while the Ig insertion subtype, specifically involving the IgL gene partner, was independently associated with poorer outcomes compared with other *MYC* SV subtypes. Although the FISH methodology failed to detect approximately 70% of all *MYC* SVs, those detected by FISH were associated with elevated *MYC* gene expression and poor outcomes suggesting a different pathogenic role for FISH-detected *MYC* subtypes compared with other *MYC* subtypes.

Conclusions: Understanding the impact of different *MYC* SVs on disease outcome is necessary for the reliable interpretation of *MYC* SVs in multiple myeloma. NGS approaches should be considered as a replacement technique for a more comprehensive evaluation of the multiple myeloma clone.

Introduction

Multiple myeloma is an incurable malignancy of plasma cells with approximately 32,000 new cases in the United States each year (1, 2). Genetic abnormalities of multiple myeloma contribute to disease heterogeneity and influence response to therapy and prognosis (1). Primary genetic abnormalities, characterized by recurrent immunoglobulin (Ig) heavy chain (IgH) structural variations (SV) and/or hyperdiploidy resulting from multiple trisomies, occur early in disease course, while secondary genetic abnormalities such as 1q gain, 17p deletion resulting in loss of *TP53*, and SVs involving the *MYC* proto-oncogene occur upon disease progression (3). Genetic events t(11;14)

(q13;q32) *CCND1/IgH*, t(6;14)(p21;q32) *CCND3/IgH* and hyperdiploidy are associated with standard risk, whereas t(4;14)(p16.3;q32) *FGFR3/MMSET/IgH*, t(14;16)(q32;q23) *IgH/MAF*, t(14;20)(q32;q12) *IgH/MAFB*, 1q gain and *TP53* deletions and single-nucleotide variants (SNV) are associated with high risk (3).

Although genetic abnormalities involving *MYC* have been documented in the progression from smoldering multiple myeloma (SMM) to multiple myeloma (4–6), the prognostic role of *MYC* SVs has not been fully established in the context of multiple myeloma. Earlier studies showed *MYC* SVs detected by FISH or target capture–based sequencing were independently associated with poor outcome (7–10). However, more recent studies using whole-genome sequencing (WGS) did not uniformly support this finding (excluding poor outcome *MYC/IgL* SVs; refs. 4, 11–13). This discrepancy is likely due to differences in methods and sensitivities of detection of *MYC* SVs by FISH or target capture–based sequencing compared with WGS. Given that *MYC* SVs often display remarkable genomic heterogeneity with numerous gene partners, reduced detection of *MYC* SVs by FISH is not unexpected (4, 8, 9, 11, 12, 14). This possibility is supported by lower frequencies of *MYC* SVs found by FISH (~13%–15%) compared with next-generation sequencing (NGS; ~23%–42%) consistent with a high false-negative rate of the *MYC* break apart (BAP) FISH probe (15). To more fully understand the role of *MYC* SVs in multiple myeloma disease outcome, we performed a retrospective study to compare the *MYC* SV subtypes identified by FISH and NGS to the expression of *MYC* and overall disease survival.

Materials and Methods

This was an institutional review board (IRB)-approved retrospective study that included newly diagnosed multiple myeloma (NDMM) cases from both the Mayo Clinic and publicly available Multiple Myeloma Research Foundation (MMRF) CoMMpass cases.

[1]Division of Laboratory Genetics, Department of Laboratory Medicine and Pathology, Mayo Clinic, Rochester, Minnesota. [2]Division of Computational Biology, Department of Quantitative Health Sciences, Mayo Clinic, Rochester, Minnesota. [3]Division of Hematology, Department of Internal Medicine, Mayo Clinic, Rochester, Minnesota. [4]Cytogenetics and Genomic Microarray Laboratory, ARUP Laboratories, Salt Lake City, Utah. [5]Division of Biomedical Statistics and Informatics, Department of Health Sciences Research, Mayo Clinic, Jacksonville, Florida. [6]Division of Hematopathology, Department of Laboratory Medicine and Pathology, Mayo Clinic, Rochester, Minnesota. [7]Division of Hematology, Department of Internal Medicine, Mayo Clinic, Scottsdale, Arizona.

Translational Relevance

Although structural variants (SV) involving *MYC* are common in multiple myeloma, the prognostic significance of different *MYC* SVs has not been clearly established. Here, we evaluated the significance of *MYC* SVs in multiple myeloma detected by next-generation sequencing (NGS) and FISH. *MYC* SVs were common and nine different subtypes could be identified by NGS. Only non-immunoglobulin (non-Ig) insertion and Ig insertion subtypes showed significant differences in outcome. Non-Ig insertion was associated with improved outcome, while the Ig insertion subtype (specifically IgL) was associated with reduced outcome. Although FISH is commonly used to detect *MYC* SVs, FISH failed to identify approximately 70% of *MYC* SVs. *MYC* SVs detected by FISH were more likely to be associated with higher *MYC* gene expression and poor outcome. Genome-wide NGS approaches should be considered as a replacement technique for a more comprehensive evaluation of the tumor clone, in comparison with traditional cytogenetic methodologies such as FISH.

Mayo clinic cohort

The Mayo Clinic (Rochester, MN campus) cohort included 1,342 unique patients with multiple myeloma seen within 90 days from diagnosis in the period from January 2006 to January 2018. Cytogenetic analysis by FISH, including the *MYC* BAP, was performed within 1 year from diagnosis and less than 6 months from the start of first-line treatment. All patients were identified using a prospectively maintained database; additional clinical and laboratory data were obtained by review of electronic medical records. All patients had authorized the use of their electronic medical record data for research. Patient samples were collected with written informed consent in accordance with recognized ethical guidelines and IRB approval. Among those patients, 140 had simultaneous data for both FISH and NGS using mate pair sequencing (MPseq).

MMRF CoMMpass cohort

The MMRF CoMMpass cohort (clinical trial identifier: NCT01454297) included 658 cases with either tumor long-insert whole-exome sequencing (WES), WGS, RNA sequencing (RNAseq) for gene expression (IA15 release), and clinical outcome data (IA16 release). The study was approved by ethics committees or IRBs at the study sites. All patients provided written informed consent in accordance with recognized ethical guidelines. RNAseq data from the CoMMpass cohort are displayed as Salmon TPM and $\log_2$-transformed $[\log_2(MYC \text{ TPM} + 0.25) - \log_2(0.25)]$ values.

FISH

FISH analysis was performed on bone marrow samples as described previously (16,17) and further described in Supplementary Methods.

DNA extraction and MPseq

DNA extraction and MPseq library preparation methods have been described previously (18–20) and further described in Supplementary Methods.

Bioinformatics and visualization

A total of 658 CoMMpass cases and 200 normal peripheral blood samples with WGS data were analyzed for breakpoint junction (SV) and copy-number abnormality (CNA). The sequencing FASTQ files were aligned to GRCh38 reference genome using BWA-MEM 0.7.17 (21). The output BAM was processed to determine coverage (reads/Kb) across the genome and normalized using a GC content and mapability (Umap k24; ref. 22) correction and then binned to 30 Kb windows. Regions of similar copy-number level were segmented using a sliding window method and then the copy-number value of each region was normalized by the mode of the coverage probability distribution function to center the values around the expected 2N level. CNA regions were calculated as any region that deviated from this expected 2N level by >10% (loss ≤ −10% deviation, gain ≥ +10% deviation). CNA of *TP53* and *CKS1B* were identified as any region that deviated from this expected 2N level by ≤1.74 as loss and ≥2.3 as gain to call *TP53* deletions and 1q gains. For SV detection, reads that mapped to locations ≥5 Kb bp apart or to different chromosomes were considered discordant. These discordant fragments were clustered by both fragment size (absolute difference in genomic positions) and midpoint (sum of genomic position). Clustering was done on both parameters using a cutoff of 5 Kb. The clusters from the normal peripheral blood WGS samples were used to create a 5 Kb mask to eliminate likely false positive from the clustering results. A further filtering was applied that required junction calls to have ≥3 supporting fragments to be called and have a genomic footprint of ≥50 bp on both sides of the junction. These SV and CNA calls were combined and visualized in a genome U-plot (19), which allowed us to interpret and characterize the *MYC* alterations into distinct structural motifs. *MYC* SV partner frequencies were calculated with R (https://www.R-project.org) and plotted using the ggplot2 library (23) or Circos (24).

ROC

The ROC curve (25) was created by plotting the false-positive rates versus true-positive rate using RNA expression level (transcription per million; TPM) and *MYC* alterations were classified using WGS data from the 658 samples from the CoMMpass cohort.

Statistical analysis

All statistical analyses were performed using statistical software JMP (Version 14.1.0, SAS Institute Inc.), SPSS15, or GraphPad Prism software and significance was determined at $P < 0.05$. Categorical variables were compared using the χ^2 test. A nonparametric (Kruskal–Wallis test) and *post hoc* (Dunn) test was used to determine difference between more than two sample groups. Overall survival (OS) was defined as time from diagnosis to death from any cause or to last follow-up, with those alive censored at date of last follow-up. Progression-free survival (PFS) was defined as the time from initiation of first-line treatment until progression or death from any cause, or last follow-up (Mayo Cohort) or from time of diagnosis until progression or death from any cause, or last follow-up (CoMMpass cohort). Survival curves were estimated using Kaplan–Meier and compared using the log-rank test. Where survival probability did not reach 0.5, mean survival times were calculated.

Data availability statement

The MPseq data that support this study have been deposited in the National Center for Biotechnology Information (NCBI)'s Sequence Read Archive with BioProject ID PRJNA739382 and can be accessed at http://www.ncbi.nlm.nih.gov/bioproject/739382. All CoMMpass data used in this study are publicly available [database of Genotypes and Phenotypes (dbGap): phs000748.v1.p1 and EGAS00001001178] and also http://www.ncbi.nlm.nih.gov/bioproject/248538.

Table 1. *MYC* subtype and expression.

	MYC subtype	Median raw TPM	Median log-transformed TPM	Total (frequency in cohort) *P* < 0.0001		Total hyperdiploidy (frequency in subtype)	
No *MYC* abnormality	No *MYC* SV	21.6	6.4	327 (49.7%)	388 (59.0%)	142 (43.4%)	165 (42.5%)
	MAX SNV	1.1	2.4	19 (2.9%)		2 (10.5%)	
	Monosomy 8	10.3	5.4	18 (2.7%)		5 (27.8%)	
	Trisomy 8	35.9	7.2	24 (3.6%)		16 (66.7%)	
MYC SV	TTD	38.3	7.3	29 (4.4%)	270 (41.0%)	22 (75.9%)	191 (70.7%)
	Terminal del	44.1	7.5	11 (1.7%)		5 (45.5%)	
	Proximal del	55.9	7.8	13 (2.0%)		7 (53.8%)	
	Ig translocation	61.5	7.9	13 (2.0%)		9 (69.2%)	
	Non-Ig insertion	68.0	8.1	65 (9.9%)		55 (84.6%)	
	Non-Ig translocation	70.8	8.1	16 (2.4%)		5 (31.3%)	
	Complex del/gain	75.0	8.2	30 (4.6%)		17 (56.7%)	
	Ig insertion	86.0	8.4	88 (13.4%)		69 (78.4%)	
	Amplification	144.1	9.2	5 (0.8%)		2 (40.0%)	
	Total	33.4	7.1	658 (100%)		356 (54.1%)	

Note: *MYC* abnormality subtype, median *MYC* TPM values, total frequency of the subtype in the CoMMpass cohort ($n = 658$), and percentage of hyperdiploidy in each *MYC* subtype. Overall *P* value (No *MYC* vs. *MYC* subtypes) determined by Kruskal–Wallis test. Individual *P* values determined by a *post hoc* Dunn test (Supplementary Table S6).

Results

Characterization of *MYC* SV subtypes

A total of 658 cases from the CoMMpass cohort with both WGS and *MYC* expression data were included, and the associated abnormality impacting the *MYC* gene region was investigated. Forty-two cases (6.4%) had a CNA involving *MYC* without a *MYC* SV, including 18 cases (2.7%) with monosomy 8 (one copy of the *MYC* gene) and 24 cases (3.6%) with trisomy 8 (three copies of the *MYC* gene; **Table 1**). Nineteen cases (2.9%) with a deleterious SNV impacting the *MAX* gene were included in a separate category given the extremely low *MYC* gene expression as previously reported (**Table 1**; ref. 4). We found 327 cases (49.7%) had neither a *MYC* SV, CNA, nor deleterious *MAX* SNV and 270 cases (41.0%) had evidence of an SV impacting the *MYC* gene region. We further categorized the cases with a *MYC* SV into nine subtypes based on the type of *MYC* SV observed (**Table 1**; Supplementary Fig. S1). These included cases with terminal tandem duplications (TTD; duplication of the genomic segment downstream of *MYC*; $n = 29$, 4.4%), terminal deletions (terminal del; deletion of the genomic segment downstream of *MYC*; $n = 11$, 1.7%), proximal deletions (proximal del; deletion of the genomic segment upstream of *MYC*; $n = 13$, 2.0%), translocations involving immunoglobulin (Ig; IgH, IgK, or IgL) enhancer sequences (Ig translocation; $n = 13$, 2.0%), templated insertions of non-Ig enhancers (non-Ig insertion; $n = 65$, 9.9%), translocations involving non-Ig enhancer sequences (non-Ig translocations; $n = 16$, 2.4%), complex deletions or gains (complex del/gain; $n = 30$, 4.6%), templated insertions of Ig (IgH, IgK, or IgL) enhancer sequences (Ig insertion; $n = 88$, 13.4%), and amplifications of *MYC* ($n = 5$, 0.8%; **Table 1**). Of 270 cases with a *MYC* SV, 37.4% involved an Ig enhancer and 62.6% involved a non-Ig enhancer. From 658 cases, 356 (54.1%) were hyperdiploid without evidence of a translocation to *CCND1, CCND3, MAF, MAFB,* or *FGFR3/MMSET*. Similar to other studies (4, 7, 9, 11, 12, 14, 26), an increase in the prevalence of hyperdiploidy in cases with a *MYC* SV was observed ($n = 191$, 70.7%), compared with cases without a *MYC* abnormality ($n = 165$, 42.5%). Specifically, cases with TTD, non-Ig insertion, and Ig insertion had an enrichment of hyperdiploidy (**Table 1**).

We compared the SVs surrounding only the *MYC* gene region of the 9 *MYC* subtypes to other established patterns of SVs recently described

in human cancers, including multiple myeloma (Supplementary Table S1; refs. 27, 28, 29). The tandem duplication (TTD) and deletion (terminal and proximal dels) subtypes were described as simple events with a single SV connecting two DNA breaks. Most ($n = 26$, 89.7%) non-Ig and Ig translocations were categorized as balanced or unbalanced translocation events with no more than 2 chromosome partners. Most ($n = 148$, 96.7%) non-Ig and Ig insertions were categorized as templated insertions, some being simple and others having evidence of complexity (Supplementary Table S1). The complex del/gains subtype involved non-Ig partners and had the most evidence of a complex rearrangement surrounding the *MYC* gene. Within this subtype, 14 (46.7%) had ≥10 SVs and these were categorized as chromothripsis similar to the definition used in ref. 29. Of the remaining 16 complex del/gain cases with 3–9 SVs around the *MYC* region, a single case was classified as having chromoplexy and the remaining 15 cases (50.0%) were termed complex, not otherwise specified. We also identified 4 (4.5%) Ig insertions subtypes as having chromothripsis and a single case as being complex, not otherwise specified (Supplementary Table S1). Three (23.1%) of the Ig translocation subtypes were also described as complex. Amplifications were defined as cases where the estimated copy number of *MYC* was ≥7N. The 5 *MYC* amplifications were achieved by either chromothripsis ($n = 4$) or aneuploidic gain or double minute ($n = 1$; Supplementary Table S1). Of 270 cases with a *MYC* SV, the most common SV category was templated insertion (54.8%; Supplementary Table S1). If eliminating simple SVs (TTD and terminal and proximal dels), the frequency of templated insertion was 68.2% of cases, similar to that reported in ref. 29.

Of 365 total *MYC* SVs identified in 270 cases with a *MYC* SV, there were 146 unique partner genes (**Fig. 1A**; Supplementary Table S2; Supplementary Fig. S2A–S2C). Although the most common gene partner involved enhancers of the following genes, IgH at 14q32.33 (13.7%), *IgL* at 22q11.22 (9.9%), *NSMCE2* at 8q24.13 (8.5%), *TXNDC5* at 6p24.3 (7.1%), *IgK* at 2p11.2 (5.5%), *FAM46C* (*TENT5C*) at 1p12 (3.0%), and *CSMD3* at 8q23.3 (2.2%), recurrent partners were found in association with specific subtypes (Supplementary Table S3). The complex del/gain subtype was enriched for *NSMCE2* and *CSMD3* partners and the proximal dels involved mostly *NSMCE2*. Although each Ig insertion case at minimum included *IgH, IgL*, or *IgK*, 55.7% of
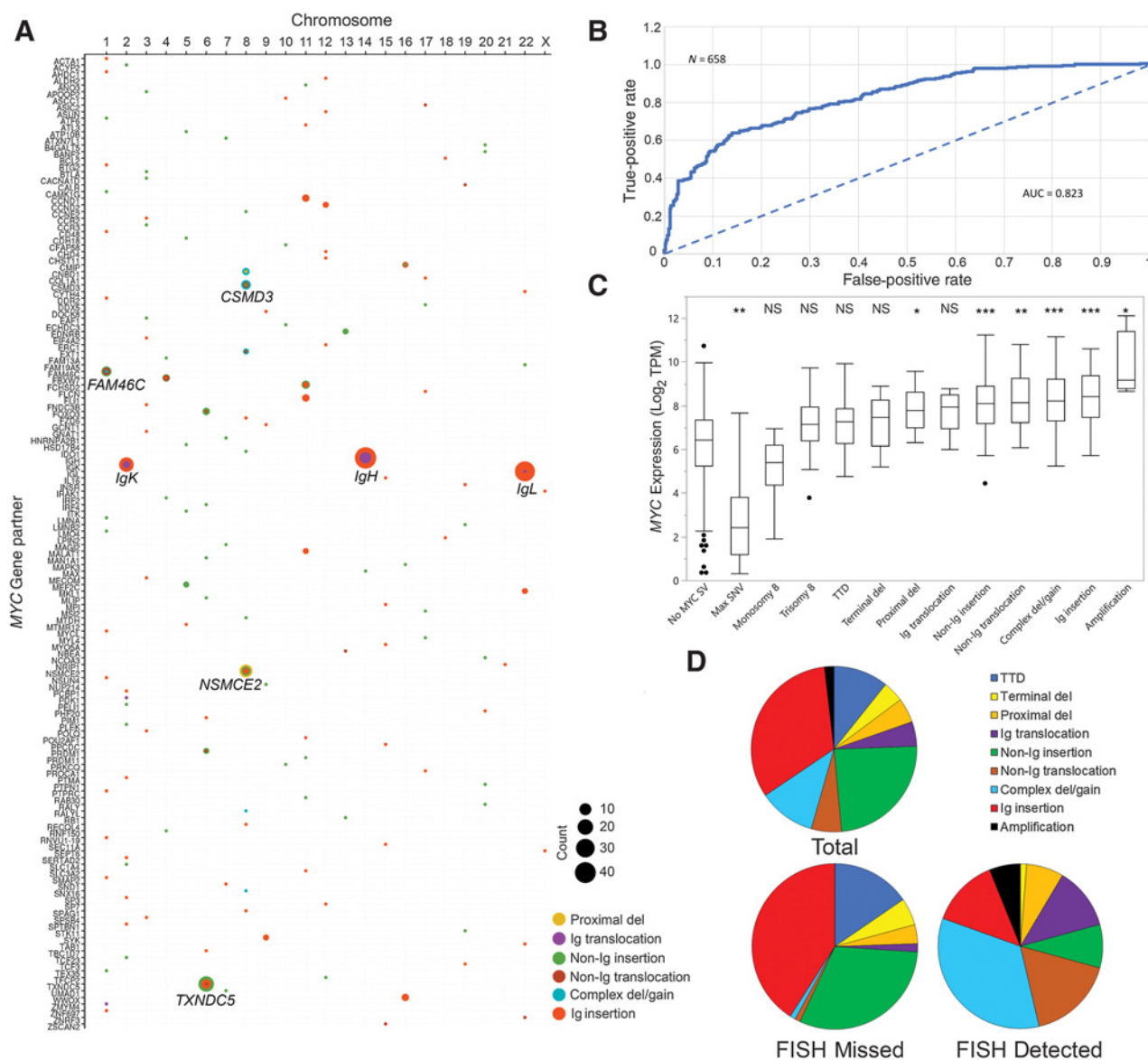
Figure 1.
MYC abnormality subtypes, partner genes, and *MYC* gene expression. **A,** Bubble plots for *MYC* SV partners. Gene name (*x*-axis) is plotted by chromosome (*y*-axis). No SV involving chromosome Y was detected. SV frequencies are indicated with circle size, and SV group by color (see legend). **B,** ROC curve for *MYC* Alteration Classification from *MYC* expression. ROC curve plotting the false-positive rate versus true-positive rate for the classification of samples for *MYC* alterations using mRNA expression levels in transcripts per million (TPM). Dotted lines give AUC = 0.5 for an uninformative classifier. **C,** Boxplot and median *MYC* transcript levels (log transform of Salmon TPM) of MMRF CoMMpass cases (*n* = 658), with observed SVs. Significant differences in each subtype were compared with the subtype with no MYC SV (***, *P* < 0.0001; **, *P* < 0.001; *, *P* < 0.05). **D,** Pie charts showing the distribution of the *MYC* SV in association with predicted FISH detection.

the cases (49/88) had three or more partners (including *MYC*) in the "templated insertion chain" involving non-Ig genes, the most common being *TXNDC5*. Of the 49 Ig insertion cases with multiple partners, 8 (16.3%) did not have a direct connection between the Ig and *MYC* gene regions, but rather were separated by a non-Ig insertion in between (5 *IgH*, 1 *IgK*, and 2 *IgL*). *TXNDC5* was the most common *MYC* partner in the non-Ig insertion subtype. The most common gene partner in non-Ig translocations was *FAM46C*. Non-Ig insertion subtype was also commonly associated with three or more partners within the "templated insertion chain" (Supplementary Table S3 and S4). No clear *MYC* partner was identified in TTD and terminal del subtypes. Similar

to Mikulasova and colleagues, (12), 57.1% of cases had two chromosome partners, 23.6% had three, 12.1% had four partners, and 7.1% had five or more partners (Supplementary Table S4). In contrast to the high frequency of *MYC* SVs, only 8 (1.2%) cases had nonsynonymous *MYC* SNVs with a median *MYC* expression of 42.9 TPM, with 6 cooccurring in cases that also had a *MYC* SV (Supplementary Table S5).

Type of *MYC* SV and association with *MYC* gene expression

We next compared *MYC* RNA levels in each *MYC* SV subtype. *MYC* RNA levels have previously been shown to correlate with the expected MYC gene signature (genes directly targeted by MYC) and a MYC gene

signature has also been shown to correlate with MYC protein levels (30, 31). These findings suggest that *MYC* RNA levels are functionally associated with the predicted effect of MYC transcription. *MYC* expression correlated with the presence of a *MYC* SV using ROC curve analysis plotting the false-positive versus true-positive rate for the classification of samples for *MYC* alterations using *MYC* TPM data. The AUC value of 0.823 suggests strong correlation of *MYC* expression with the presence of a *MYC* SV (**Fig. 1B**). Significant differences in *MYC* expression were also observed in some *MYC* SV subtypes compared with cases without a *MYC* SV (**Fig. 1C**; **Table 1**; Supplementary Table S6). Lowest median *MYC* expression was observed in cases with a *MAX* SNV (1.1 TPM) or monosomy 8 (10.3 TPM). The 327 cases with no *MYC* SV had a median *MYC* expression of 21.6 TPM. Compared with cases with no *MYC* SV, expression of *MYC* was significantly increased in cases with prox- imal del (55.9 TPM), non-Ig insertion (68.0 TPM), non-Ig trans- location (70.8 TPM), complex del/gain (75.0 TPM), Ig insertion (86.0 TPM), and amplification (144.1 TPM) and was significantly reduced in cases with a *MAX* SNV (**Fig. 1C**; **Table 1**; Supplementary Table S6). Significant differences in *MYC* expression were not iden- tified between cases with no *MYC* SV and monosomy 8, trisomy 8, TTD, terminal del, and Ig translocations and between many of the individual *MYC* SV subtypes (Supplementary Table S6).

Type of *MYC* SV and detection by FISH

Given the heterogeneity of the *MYC* SVs identified by NGS and our previous observation of reduced detection of *MYC* SVs by *MYC* BAP FISH compared with NGS (15), we evaluated which *MYC* SVs give an abnormal *MYC* BAP FISH result using our Mayo Clinic cohort with MPseq and FISH data ($n = 140$). Similar to Abdallah and collea- gues (16), 7 cases (5.0%) were abnormal using the *MYC* BAP FISH probe while 41 cases (29.3%) were abnormal by MPseq. Using MPseq and FISH data described in Smadbeck and colleagues (15), subtypes more likely to be undetected by FISH include proximal deletions and non-Ig and Ig insertions (Supplementary Table S7; Supplementary Fig. S3).

We next analyzed 658 CoMMpass cases with the goal to infer, based on visualization of the genomic architecture from WGS and knowl- edge of the location of the *MYC* BAP FISH probes, whether a *MYC* SV could be detected by FISH. Using this approach, we predicted a *MYC* SV could be detected by FISH in 82/658 (12.5%) cases, similar to the approximately 13%–15% detected using *MYC* FISH in previous studies (32, 33). We predicted the *MYC* BAP FISH probe would miss approximately 69.6% of all *MYC* SVs and would have reduced sensitivity in detecting TTD, terminal deletions, non-Ig insertions, and Ig insertions (Supplementary Table S8; **Fig. 1D**). FISH was predicted to detect most amplifications, complex deletion/duplica- tions, most non-Ig and Ig translocations, and some non-Ig and Ig insertions (Supplementary Table S8; **Fig. 1D**). Of cases with hyperdi- ploidy, 75.4% had a *MYC* SV predicted to be missed by FISH. Cases with *MYC* SVs predicted to be missed by FISH had a slightly lower *MYC* gene expression (63.7 TPM, range: 5.2–611.5 TPM) compared with cases predicted to be detected by FISH (80.1 TPM, range: 8.9– 1,111.8 TPM; $P = 0.119$; Supplementary Table S8).

MYC gene expression and patient survival

We next evaluated whether elevated *MYC* gene expression, irre- spective of *MYC* SV status, was associated with differences in patient survival. Boxplot analysis was used to categorize *MYC* expression in 631 CoMMpass cases with available OS and *MYC* expression data. Top quartile/high *MYC* expression was defined as *MYC* expression ≥75.0

TPM, and bottom quartile/low *MYC* expression was defined as ≤16.5 TPM. Although mean OS and PFS was shorter in patients with high *MYC* expression compared with patients with low *MYC* expression (OS: 4.6 years vs. 5.3 years, $P = 0.038$; PFS: 2.5 years vs. 3.1 years, $P = 0.068$; **Fig. 2A** and **B**), the findings were only significant for OS. Using *MYC* expression as a continuous variable, high *MYC* expression was associated with an increased risk of death on univariate analysis ($P = 0.027$), but this was not considered significant in a multivariate model including *MYC* expression and other high-risk abnormalities such as *TP53* deletion; 1q gain; high-risk translocations t(4;14), t(14;16) and t(14;20); ISS stage III; and ≥70 years of age (**Table 2**). Similar observations were observed when analyzing *MYC* as a categorical variable (high vs. low/medium *MYC* expression) in the full cohort (Supplementary Table S9). High *MYC* expression was significantly associated with inferior OS in cases classified as nonhyperdiploid ($P = 0.001$), but not in cases classified as hyperdiploid ($P = 0.843$; Sup- plementary Fig. S4).

Although median age was similar among cases with high *MYC* expression (64 years) compared with low *MYC* expression (63 years), cases with high *MYC* expression had an increased frequency of *TP53* deletion (14.5%), 1q gain (48.0%), and ISS stage III (36.0%) compared with cases with low *MYC* expression (8.0% with *TP53* deletion, 24.1% with 1q gain, 25.4% ISS stage III). Low *MYC* expression was associated with a low frequency of any *MYC* SV (8.6%), including *MYC*/IgL SVs (1.1%; **Fig. 2C**; Supplementary Table S10). Of cases with a *MYC* SV present in the low *MYC* expression group, 3.2% were TTD, 2.1% were non-Ig insertion, 0.5% had a complex del/gain, and 1.1% had an Ig insertion. In contrast, 80.2% of cases in the high *MYC* expression group had evidence of a *MYC* SV. The most common *MYC* SV in this group included Ig insertion (33.8%), with 35% of these Ig insertion cases involving IgL. Twenty-six cases (17.2%) with high *MYC* expres- sion had no *MYC* abnormality detected (**Fig. 2C**; Supplementary Table S10).

MYC SVs detected by FISH, but not by NGS, are associated with poor survival outcome

We compared the impact of *MYC* SVs on patient survival when detected by FISH or NGS. We recently reported that diseased survival was shorter in patients with a *MYC* SV compared with patients without a *MYC* SV using the *MYC* BAP FISH probe (5.3 vs. 8.0 years, $P < 0.001$; ref. 16). Among patients with hyperdiploidy, OS was decreased in patients with a *MYC* SV detected by FISH compared with those without a *MYC* SV (5.7 vs. 8.6 years, $P = 0.007$; **Fig. 3A**). Similarly, among patients without hyperdiploidy, OS was decreased in patients with a *MYC* SV detected by FISH compared with those without a *MYC* SV (2.8 vs. 6.8 years, $P < 0.0001$; **Fig. 3B**). However, among patients with hyperdiploidy, PFS was similar to those with a *MYC* SV detected by FISH compared with those without a *MYC* SV (4.4 vs. 4.3 years, $P = 0.680$; **Fig. 3C**). In contrast, among patients without hyperdiploidy, PFS was decreased in those with a *MYC* SV detected by FISH compared with those without a *MYC* SV (2.6 vs. 3.5 years, $P < 0.001$; **Fig. 3D**).

In contrast, there was no significant difference in OS and PFS between patients from the Mayo cohort with a *MYC* SV detected by MPseq compared with those without a *MYC* SV (OS: 7.7 vs. 6.9 years, $P = 0.990$ and PFS: 2.5 and 3.0 years, $P = 0.490$; **Fig. 3E** and **F**). Similarly, there was no significant difference in OS and PFS between patients from the CoMMpass cohort with a *MYC* SV detected by WGS compared with those without a *MYC* SV (OS: 5.7 and 5.5 years, $P = 0.415$; PFS: 3.3 and 3.1 years, $P = 0.755$; **Fig. 3G** and **H**). Although no significant differences in OS and PFS between patients with a *MYC* SV and those without a *MYC* SV were observed, a trend toward improved
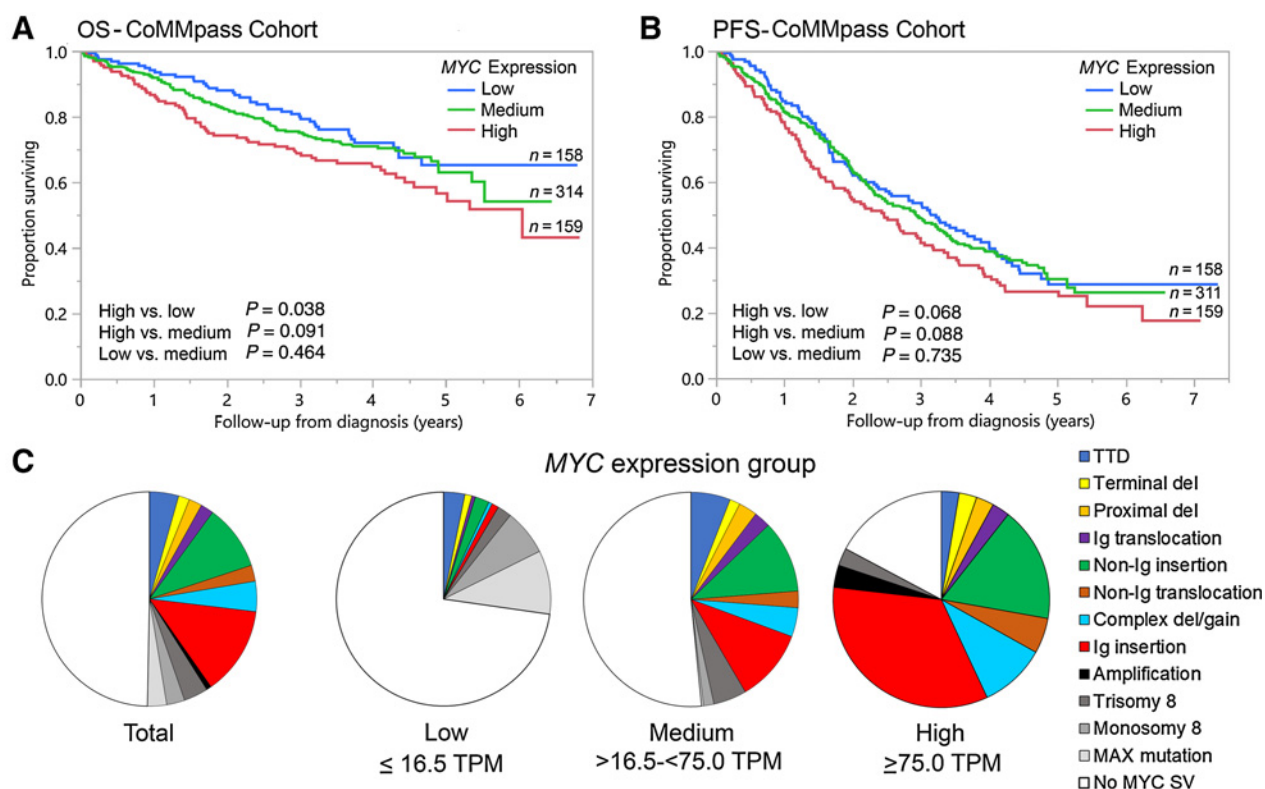
Figure 2.
Impact of *MYC* gene expression on OS and PFS. **A,** A comparison of OS (years) in patients with low *MYC* expression (≤16.5 TPM; blue line), medium *MYC* expression (16.5–75 TPM; green line), and high *MYC* expression (≥75.0 TPM; red line) detected by RNAseq from the CoMMpass cohort. OS time (mean) was 5.3 years [95% confidence interval (CI): 5.0–5.7], 4.8 years (95% CI: 4.6–5.1), and 4.6 years (95% CI: 4.2–5.0) in low (*n* = 158), medium (*n* = 314), and high (*n* = 159) *MYC* expression cohorts, respectively. **B,** A comparison of PFS (years) in patients with low *MYC* expression (≤16.5 TPM; blue line), medium *MYC* expression (16.5–75 TPM; green line), and high *MYC* expression (≥75.0 TPM; red line) detected by RNAseq from the CoMMpass cohort. PFS time (median) was 3.1 years (95% CI: 2.4–3.9), 2.9 years (95% CI: 2.4–3.3), and 2.5 years (95% CI: 1.7–3.0) in low (*n* = 158), medium (*n* = 311), and high (*n* = 159) *MYC* expression cohorts, respectively. **C,** Pie charts showing the distribution of the *MYC* SV in association with *MYC* gene expression.

OS and PFS was identified in the hyperdiploid cohort in contrast to the nonhyperdiploid cohort (Supplementary Fig. S5).

Although evaluation of all *MYC* SVs together resulted in no significant differences in OS and PFS compared with cases with no *MYC* SVs, the impact of individual *MYC* SV subtypes on OS and PFS was further evaluated. Among the nine *MYC* SV subtypes, only non-Ig insertion and Ig insertion subtypes showed significant differences in either OS and/or PFS in univariate analysis (Supplementary Table S11). Patients with non-Ig insertion subtype had improved OS and PFS, while patients with Ig insertion had reduced OS and PFS (**Fig. 4**; Supplementary Fig. S6). Non-Ig insertion subtype was associated with improved OS [risk ratio (RR) 0.33, *P* = 0.004] and PFS (RR 0.60, *P* = 0.018), while Ig insertion subtype was associated with reduced PFS (RR 1.46, *P* = 0.016) on univariate analysis (Supplementary Tables S12 and S13). Among the Ig insertion subtype, only those involving the IgL gene partner were associated with reduced PFS (RR 2.12, *P* < 0.001) on univariate analysis (Supplementary Table S14). In a multivariate model including non-Ig insertion and the favorable risk category of hyperdiploidy, non-Ig insertion retained its prognostic value at predicting OS and PFS (OS RR 0.32, *P* = 0.005; PFS RR 0.60, *P* = 0.025; Supplementary Table S12). In a multivariate model including either Ig insertion or IgL SVs (all IgL insertions) and other high-risk abnormalities, both Ig insertion and IgL SVs retained their

prognostic significance at predicting PFS (Ig insertion, RR 1.40, *P* = 0.042; IgL, RR 2.29, *P* < 0.001; Supplementary Tables S13 and S14), with a trend toward reduced OS and PFS in Ig insertion subtypes with increased *MYC* partners (Supplementary Fig. S7).

Discussion

SVs involving the *MYC* proto-oncogene are common secondary events in multiple myeloma and are associated with SMM to multiple myeloma disease progression (4–6, 8, 9, 11–14). We observed *MYC* SVs in 41% of multiple myeloma cases detected by WGS and similar to other studies, WGS identified a greater frequency of *MYC* SVs compared with FISH (4, 11–13). Among the nine *MYC* SV subtypes, the non-Ig insertion and Ig insertion subtypes, namely IgL insertions, showed significant differences in outcome in comparison with cases without a *MYC* SV, similar to other studies (4, 11, 12). The non-Ig insertion subtype was associated with improved outcomes, while the Ig insertion subtype (specifically when partnered with IgL) was associated with poor outcomes. Thus, *MYC* appears to be associated with poor outcome only when partnered with IgL. The main driver is likely the association with IgL as IgL SVs, even in the absence of partnering with *MYC*, are associated with poor outcome (11). The poor outcome associated with IgL SVs has been proposed to involve the strong

Table 2. The influence of *MYC* expression, *TP53* deletion, 1q gain, high-risk translocations, ISS stage, patient age, and hyperdiploidy on OS and PFS.

Independent variables	Univariate model (OS)				Multivariate model (OS)				Univariate model (PFS)				Multivariate model (PFS)			
	RR	P value	Lower 95%	Upper 95%	RR	P value	Lower 95%	Upper 95%	RR	P value	Lower 95%	Upper 95%	RR	P value	Lower 95%	Upper 95%
MYC expression continuous	1.002	0.027	1.000	1.003	1.001	0.070	1.000	1.003	1.001	0.051	1.000	1.002	1.001	0.136	1.000	1.002
TP53 deletion yes vs. no	1.736	0.008	1.152	2.617	1.789	0.006	1.182	2.701	1.454	0.027	1.043	2.027	1.524	0.016	1.081	2.152
1q gain yes vs. no	1.677	<0.001	1.246	2.259	1.440	0.025	1.047	1.980	1.568	<0.001	1.251	1.966	1.393	0.008	1.092	1.777
High-risk translocations yes vs. no	1.416	0.066	0.978	2.051	1.614	0.017	1.088	2.393	1.425	0.014	1.075	1.890	1.432	0.019	1.062	1.932
ISS III vs. I/II	2.134	<0.001	1.571	2.898	1.786	<0.001	1.301	2.453	1.622	<0.001	1.278	2.058	1.462	0.002	1.145	1.867
Age group ≥ 70 vs.<70	2.259	<0.001	1.676	3.044	2.024	<0.001	1.470	2.787	1.623	<0.001	1.287	2.048	1.514	0.001	1.183	1.934
MYC expression continuous	1.002	0.027	1.000	1.003	1.002	0.019	1.000	1.003	1.001	0.051	1.000	1.002	1.001	0.034	1.000	1.002
Hyperdiploid yes vs. no	0.910	0.535	0.677	1.224	0.875	0.376	0.650	1.177	0.885	0.283	0.709	1.11	0.864	0.200	0.662	1.080

Note: Comparison of *MYC* expression as a continuous variable in full cohort on OS and PFS in two models (model 1: evaluation of high-risk abnormalities, model 2: evaluation of hyperdiploidy). *TP53* deletion yes vs. no; 1q gain (greater than two copies of 1q including the *CKS1B* gene) yes vs. no; high-risk IgH translocations (t(4;14), t(14;16), or t(14;20)) yes vs. no; ISS stage III vs. I/II; and ≥70 years vs. <70 years of age at diagnosis. *P* value determined using Wald test. Risk ratio for *MYC* indicated as unit risk ratio, per unit change in regressor. Risk ratios that are considered significant (*P* < 0.05) are indicated in red. RR, Risk ratio. *N* = 545 for univariate OS, *N* = 523 for multivariate OS, *N* = 542 for univariate PFS, *N* = 521 for multivariate PFS.

association of the IKZF1 transcription factor to the IgL locus rendering cases with IgL SVs less sensitive to immunomodulatory drug treatment (11). How the non-Ig insertion subtype confers a prognostic benefit independent of hyperdiploidy remains unknown.

Within clinical genomics laboratories, *MYC* SVs are most often identified using BAP FISH probes spanning the *MYC* genomic region. FISH detects approximately 13%–15% of *MYC* SVs in newly diagnosed multiple myeloma (32, 33), compared with approximately 23%–42% detected by WGS (4, 11–13). FISH underestimates the frequency of *MYC* SVs in multiple myeloma by about 2–3 fold (4, 8, 12, 15), likely due to the heterogeneity of *MYC* SV breakpoints. This makes the design of FISH probes capable of capturing all *MYC* SVs a significant challenge. Similar to multiple myeloma, approximately 32% of diffuse large B-cell lymphomas were also discordant between FISH and a hybrid-capture sequencing assay (34). Most of these discordant cases had non-Ig partners with breakpoints outside of the genic cluster (34). Most of the cases with non-Ig SVs represented high-grade B-cell lymphomas, a WHO entity that requires correct *MYC* classification for accurate diagnosis and patient management. Understanding the limitations of the *MYC* BAP probe is critical because clinical laboratories use FISH for the evaluation of *MYC* SVs and evidence of false-negative *MYC* BAP FISH results have been reported (15, 35–38). We show that FISH has reduced sensitivity toward non-Ig and Ig insertion subtypes because these rearrangements often occur between the 5′ and 3′ *MYC* FISH probes and do not always result in a separated 5′ and 3′ FISH pattern. Although the *MYC* FISH probe fails to detect approximately 70% of *MYC* SVs that are detected by NGS, the *MYC* probe can still identify *MYC* SVs in approximately 12% of patients with multiple myeloma. *MYC* SVs detected by FISH have a higher gene expression and are more likely to be associated with poor outcome suggesting a different pathogenic role compared with other MYC SVs.

Older studies using FISH or target capture–based sequencing found that *MYC* SVs were associated with inferior survival (7–10). Another study identified *MYC* SVs in 13% of patients with multiple myeloma with no correlation with other primary abnormalities and no prognostic impact on survival (33). Whether these findings are explained by differences in *MYC* probe placement or differences in the proportion of hyperdiploidy to nonhyperdiploidy is uncertain. Other studies also found no difference in outcome between cases with or without *MYC* SVs detected using WGS. Although *MYC* SVs are more common in hyperdiploidy (4, 7, 9, 11, 12, 14, 26), the influence of *MYC* SVs on survival in this group has been unclear. While previous studies have shown that FISH-detected *MYC* SVs are associated with poor outcome only in the hyperdiploid group (7), our findings suggest that FISH-detected *MYC* SVs and also high *MYC* expression may be more predictive of poor outcome in the nonhyperdiploid group. It is possible that differences in the frequency and ratio of the favorable non-Ig insertion to the unfavorable Ig insertion subtype between hyperdiploid and nonhyperdiploid groups (Supplementary Fig. S8) may explain some of the differences in outcomes between these cohorts when evaluating *MYC* SVs.

Previous studies have shown that *MYC* expression levels correlate with an expected MYC gene signature (30). A MYC signature has also been shown to correlate with MYC protein levels detected by IHC (31), providing support that *MYC* RNA levels are associated with the predicted effect of MYC transcription. *MYC* overexpression using IHC has been identified in approximately 40% of patients with multiple myeloma, similar to the frequency of *MYC* SVs identified in this study, and was associated with reduced survival (39, 40). We also observe that increased *MYC* expression was independently associated with poorer OS, but primarily in nonhyperdiploid cases. These
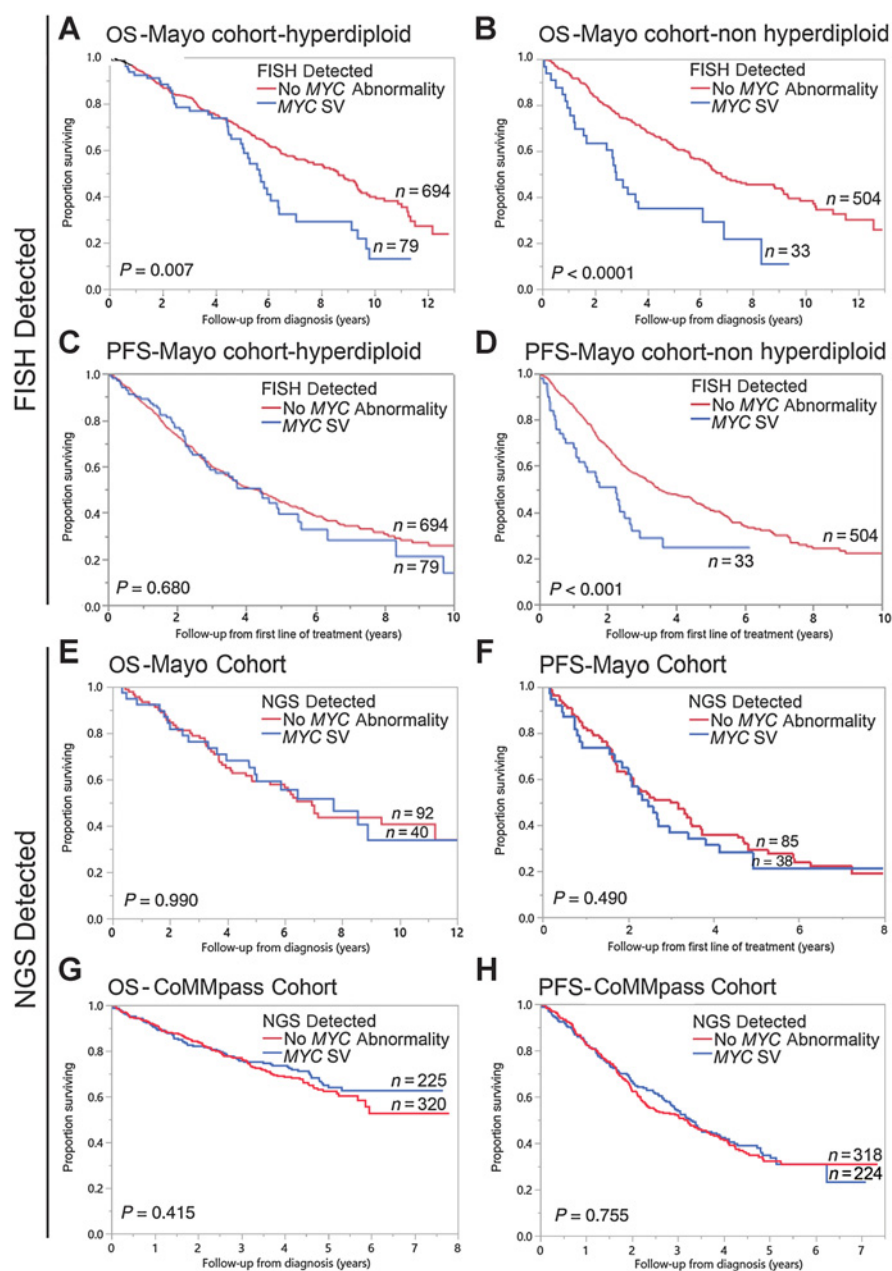
Figure 3.
Impact of *MYC* SV detected by FISH or NGS on OS and PFS. A comparison of OS (years) in patients with a *MYC* SV detected by FISH (blue curve), and patients without *MYC* SV (red curve) among patients with hyperdiploidy in **A** or among patients without hyperdiploidy in **B** from the Mayo Cohort. OS time (median) in the hyperdiploid group was 5.7 (95% CI: 5.0–6.4) years (*n* = 79) and 8.6 (95% CI: 7.5–9.3) years (*n* = 694) in the *MYC* SV and no *MYC* SV groups, respectively. OS time (median) in the nonhyperdiploid group was 2.8 (95% CI: 1.5–6.1) years (*n* = 33) and 6.8 (95% CI: 6.2–8.8) years (*n* = 504) in the *MYC* SV and no *MYC* SV groups, respectively. A comparison of PFS (years) in patients with a *MYC* SV detected by FISH (blue curve), and patients without *MYC* SV (red curve) among patients with hyperdiploidy in **C** or among patients without hyperdiploidy in **D** from the Mayo Cohort. PFS time (median) in the hyperdiploid group was 4.4 (95% CI: 2.9–5.5) years (*n* = 79) and 4.3 (95% CI: 3.7–4.9) years (*n* = 694) in the *MYC* SV and no *MYC* SV groups, respectively. PFS time (median) in the nonhyperdiploid group was 2.6 (95% CI: 1.1–2.7) years (*n* = 33) and 3.5 (95% CI: 3.1–4.5) years (*n* = 504) in the *MYC* SV and no *MYC* SV groups, respectively. **E,** A comparison of OS (years) in patients with *MYC* SV detected by MPseq (blue curve) and patients without a *MYC* SV detected by MPseq (red curve) from the Mayo cohort. OS time (median) was 7.7 (95% CI: 4.8–not reached) years (*n* = 40) and 6.9 (95% CI: 4.8–11.2) years (*n* = 92) in the two groups, respectively. **F,** A comparison of PFS (years) in patients with *MYC* SV detected by MPseq (blue curve) and patients without *MYC* SV detected by MPseq (red curve) from the Mayo cohort. PFS time (median) was 2.5 (95% CI: 1.9–3.4) years (*n* = 38) and 3.0 (95% CI: 2.1–3.5) years (*n* = 85) in the two groups, respectively. **G,** A comparison of OS (years) in patients with a *MYC* SV detected by WGS (blue curve) and patients without a *MYC* SV detected by WGS (red curve) from the CoMMpass cohort. OS time (mean) was 5.7 (95% CI: 5.3–6.1) years (*n* = 225) and 5.5 (95% CI: 5.2–5.9) years (*n* = 320) in the *MYC* SV and no *MYC* SV groups, respectively. **H,** A comparison of PFS (years) in patients with *MYC* SV detected by WGS (blue curve) and patients without a *MYC* SV detected by WGS (red curve) from the CoMMpass cohort. PFS time (median) was 3.3 (95% CI: 2.8–3.9) years (*n* = 224) and 3.1 (95% CI: 2.3–3.7) years (*n* = 318) in the *MYC* SV and no *MYC* SV groups, respectively.
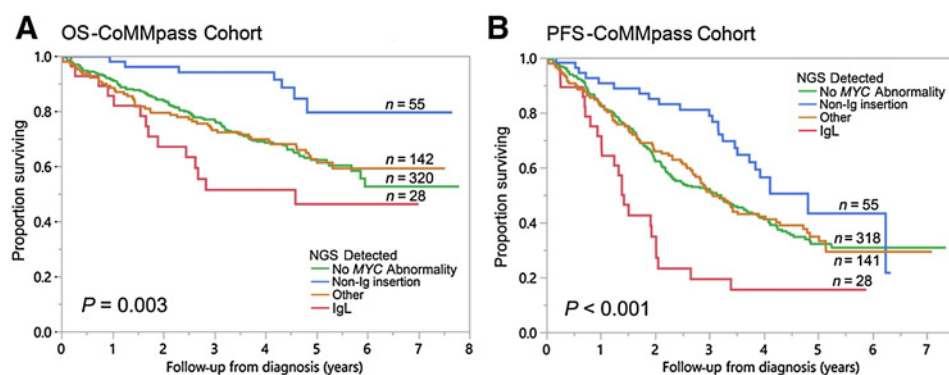
Figure 4.
Impact of different *MYC* SVs detected by NGS on OS and PFS. **A,** A comparison of OS (years) in patients with no *MYC* abnormality (no *MYC* SV, *MAX* SNV, monosomy 8, and trisomy 8; green line), patients with non-Ig insertion (blue line), patients with IgL rearrangements (all IgL insertions; red line), and all others (orange line) detected by WGS from the CoMMpass cohort. OS time (mean) was 5.5 (95% CI: 5.2–5.9) years ($n = 320$), 6.9 (95% CI: 6.3–7.4) years ($n = 55$), 4.3 (95% CI: 3.2–5.3) years ($n = 28$), and 5.4 (95% CI: 4.9–5.9) years ($n = 142$) in the no *MYC* abnormality, non-Ig insertion, IgL, and other group, respectively. **B,** A comparison of PFS (years) in patients with no *MYC* abnormality (no *MYC* SV, *MAX* SNV, monosomy 8, and trisomy 8; green line), patients with non-Ig insertion (blue line), patients with IgL rearrangements (all Ig insertions; red line), and all others (orange line) detected by WGS from the CoMMpass cohort. PFS time (median) was 3.2 (95% CI: 2.4–3.9) years ($n = 318$), 4.8 (95% CI: 3.6–6.1) years ($n = 55$), 1.4 (95% CI: 1.2–1.6) years ($n = 28$), and 3.1 (95% CI: 2.6–3.5) years ($n = 141$) in the no *MYC* abnormality, non-Ig insertion, IgL, and other group, respectively.

differences may be explained by the reduced frequency of the non-Ig insertion subtype in the nonhyperdiploid group. We also observed 26 cases (4%) had high *MYC* expression without evidence of a *MYC* SV. This finding may be due to epigenetic factors, other SNVs, a *MYC* SV not detected by NGS, or by increased signaling from a pathway such as NF-κB that promotes *MYC* expression (41). Elevated *BIRC3, NFKB2,* and *NFKBIA* expression was observed in cases with high *MYC* expression without a *MYC* SV (data not shown), consistent with a linear relationship between *MYC* expression and NF-κB index in cases without a *MYC* SV (4). Although high *MYC* expression in this subtype with no *MYC* SV showed a trend toward reduced survival, the sample size was small and results were not considered significant ($P = 0.234$; data not shown). While expression microarray or RNAseq has been proposed in the evaluation of multiple myeloma (42), this approach has not been uniformly applied into clinical practice and the relative instability of RNA compared with DNA-based genetic tests can be problematic. Evaluation of MYC protein levels by IHC has also not always correlated with the presence of *MYC* SVs detected by FISH raising the concern that IHC may not be sensitive enough to function as a surrogate for *MYC* SVs (43), a finding that is not surprising given the challenges of detecting *MYC* SVs by FISH.

This study is limited by its retrospective nature and by the heterogeneity in treatment regimens in both cohorts. In addition, our sample size for cases with MPseq results was limited; however, the results were consistent with the much larger CoMMpass cohort. Another limitation is the lack of available *MYC* FISH data and the reliance on inferring the FISH result from our training set that included NGS and FISH data from 70 previous cases from Smadbeck and colleagues (15).

In summary, we show that non-Ig insertion *MYC* subtypes are associated with improved outcomes and Ig insertion *MYC* subtypes (specifically those involving IgL) are associated with poor outcomes. Although the *MYC* BAP FISH approach has the potential to miss nearly 70% of *MYC* SVs demonstrating that NGS appears to be a more robust technique to characterize a greater fraction of *MYC* SVs, FISH can identify *MYC* SVs associated with higher gene expression and poorer outcome. In addition to identifying a greater fraction of *MYC*

SVs, NGS has the potential to identify other clinically significant SVs, CNAs, and SNVs that are currently not routinely evaluated in clinical genomics laboratories. Although NGS is currently associated with increased costs, longer assay turnaround times, greater analysis complexities, and increased data storage requirements compared with FISH (15), NGS approaches should be evaluated as a replacement technique for a more comprehensive evaluation of the tumor clone, in comparison with traditional cytogenetic methodologies such as FISH.

Authors' Disclosures

Authors' Contributions

N. Sharma: Data curation, formal analysis, writing–review and editing. **J.B. Smadbeck:** Data curation, software, formal analysis, writing–review and editing. **N. Abdallah:** Data curation, software, formal analysis, writing–review and editing. **C. Zepeda-Mendoza:** Data curation, software, formal analysis, writing–review and editing. **M. Binder:** Formal analysis. **K.E. Pearce:** Resources. **Y.W. Asmann:** Resources. **J.F. Peterson:** Writing–review and editing. **R.P. Ketterling:** Writing–review and editing. **P.T. Greipp:** Writing–review and editing. **P.L. Bergsagel:** Conceptualization, resources. **S.V. Rajkumar:** Resources. **S.K. Kumar:** Resources, writing–review and editing. **L.B. Baughn:** Conceptualization, data curation, formal analysis, supervision, methodology, writing–original draft, project administration, writing–review and editing.

Acknowledgments

References

1. Rajkumar SV. Multiple myeloma: 2020 update on diagnosis, risk-stratification and management. Am J Hematol 2020;95:548–67.
2. Siegel RL, Miller KD, Jemal A. Cancer statistics. CA Cancer J Clin 2020;70:7–30.
3. Kumar SK, Rajkumar SV. The multiple myelomas - current concepts in cytogenetic classification and therapy. Nat Rev Clin Oncol 2018;15:409–21.
4. Misund K, Keane N, Stein CK, Asmann YW, Day G, Welsh S, et al. MYC dysregulation in the progression of multiple myeloma. Leukemia 2020;34:322–6.
5. Shou Y, Martelli ML, Gabrea A, Qi Y, Brents LA, Roschke A, et al. Diverse karyotypic abnormalities of the c-myc locus associated with c-myc dysregulation and tumor progression in multiple myeloma. Proc Natl Acad Sci U S A 2000;97: 228–33.
6. Chiecchio L, Dagrada GP, Protheroe RK, Stockley DM, Smith AG, Orchard KH, et al. Loss of 1p and rearrangement of MYC are associated with progression of smouldering myeloma to myeloma: sequential analysis of a single case. Haematologica 2009;94:1024–8.
7. Weinhold N, Kirn D, Seckinger A, Hielscher T, Granzow M, Bertsch U, et al. Concomitant gain of 1q21 and MYC translocation define a poor prognostic subgroup of hyperdiploid multiple myeloma. Haematologica 2016;101:e116–9.
8. Walker BA, Wardell CP, Brioli A, Boyle E, Kaiser MF, Begum DB, et al. Translocations at 8q24 juxtapose MYC with genes that harbor superenhancers resulting in overexpression and poor prognosis in myeloma patients. Blood Cancer J 2014;4:e191.
9. Walker BA, Wardell CP, Murison A, Boyle EM, Begum DB, Dahir NM, et al. APOBEC family mutational signatures are associated with poor prognosis translocations in multiple myeloma. Nat Commun 2015;6:6997.
10. Glitza IC, Lu G, Shah R, Bashir Q, Shah N, Champlin RE, et al. Chromosome 8q24.1/c-MYC abnormality: a marker for high-risk myeloma. Leuk Lymphoma 2015;56:602–7.
11. Barwick BG, Neri P, Bahlis NJ, Nooka AK, Dhodapkar MV, Jaye DL, et al. Multiple myeloma immunoglobulin lambda translocations portend poor prognosis. Nat Commun 2019;10:1911.
12. Mikulasova A, Ashby C, Tytarenko RG, Qu P, Rosenthal A, Dent JA, et al. Microhomology-mediated end joining drives complex rearrangements and overexpression of MYC and PVT1 in multiple myeloma. Haematologica 2020;105:1055–66.
13. Walker BA, Mavrommatis K, Wardell CP, Ashby TC, Bauer M, Davies F, et al. A high-risk, double-hit, group of newly diagnosed myeloma identified by genomic analysis. Leukemia 2019;33:159–70.
14. Affer M, Chesi M, Chen WG, Keats JJ, Demchenko YN, Roschke AV, et al. Promiscuous MYC locus rearrangements hijack enhancers but mostly superenhancers to dysregulate MYC expression in multiple myeloma. Leukemia 2014; 28:1725–35.
15. Smadbeck JB, Peterson JF, Pearce K, Pitel BA, Figueroa AL, Timm M, et al. Mate pair sequencing outperforms fluorescence in situ hybridization in the genomic characterization of multiple myeloma. Blood Cancer J 2019;9:103.
16. Abdallah N, Baughn LB, Rajkumar SV, Kapoor P, Gertz MA, Dispenzieri A, et al. Implications of MYC rearrangements in newly diagnosed multiple myeloma. Clin Cancer Res 2020;26:6581–88.
17. Baughn LB, Pearce K, Larson D, Polley MY, Elhaik E, Baird M, et al. Differences in genomic abnormalities among African individuals with monoclonal gammopathies using calculated ancestry. Blood Cancer J 2018;8:96.
18. Smadbeck JB, Johnson SH, Smoley SA, Gaitatzes A, Drucker TM, Zenka RM, et al. Copy number variant analysis using genome-wide mate-pair sequencing. Genes Chromosomes Cancer 2018;57:459–70.
19. Gaitatzes A, Johnson SH, Smadbeck JB, Vasmatzis G. Genome U-Plot: a whole genome visualization. Bioinformatics 2018;34:1629–34.
20. Aypar U, Smoley SA, Pitel BA, Pearce KE, Zenka RM, Vasmatzis G, et al. Mate pair sequencing improves detection of genomic abnormalities in acute myeloid leukemia. Eur J Haematol 2019;102:87–96.
21. Heng L. Aligning sequence reads, clone sequences and assembly contigs with BWA-MEM. arXiv 2013. Available from: https://arxiv.org/abs/1303.3997.
22. Karimzadeh M, Ernst C, Kundaje A, Hoffman MM. Umap and bismap: quantifying genome and methylome mappability. Nucleic Acids Res 2018;46: e120.
23. Wickham H. Ggplot2: elegant graphics for data analysis. New York, NY: Springer-Verlag; 2009. p VIII, 213.
24. Krzywinski M, Schein J, Birol I, Connors J, Gascoyne R, Horsman D, et al. Circos: an information aesthetic for comparative genomics. Genome Res 2009; 19:1639–45.
25. Mandrekar JN. Receiver operating characteristic curve in diagnostic test assessment. J Thorac Oncol 2010;5:1315–6.
26. Walker BA, Mavrommatis K, Wardell CP, Ashby TC, Bauer M, Davies FE, et al. Identification of novel mutational drivers reveals oncogene dependencies in multiple myeloma. Blood 2018;132:587–97.
27. Li Y, Roberts ND, Wala JA, Shapira O, Schumacher SE, Kumar K, et al. Patterns of somatic structural variation in human cancer genomes. Nature 2020;578: 112–21.
28. Hadi K, Yao X, Behr JM, Deshpande A, Xanthopoulakis C, Tian H, et al. Distinct classes of complex structural variation uncovered across thousands of cancer genome graphs. Cell 2020;183:197–210.
29. Rustad EH, Yellapantula VD, Glodzik D, Maclachlan KH, Diamond B, Boyle EM, et al. Revealing the impact of structural variants in multiple myeloma. Blood Cancer Discov 2020;1:258–73.
30. Chesi M, Robbiani DF, Sebag M, Chng WJ, Affer M, Tiedemann R, et al. AID-dependent activation of a MYC transgene induces multiple myeloma in a conditional mouse model of post-germinal center malignancies. Cancer Cell 2008;13:167–80.
31. Chng WJ, Huang GF, Chung TH, Ng SB, Gonzalez-Paz N, Troska-Price T, et al. Clinical and biological implications of MYC activation: a common difference between MGUS and newly diagnosed multiple myeloma. Leukemia 2011;25: 1026–35.
32. Avet-Loiseau H, Gerson F, Magrangeas F, Minvielle S, Harousseau JL, Bataille R, et al. Rearrangements of the c-myc oncogene are present in 15% of primary human multiple myeloma tumors. Blood 2001;98:3082–6.
33. Avet-Loiseau H, Attal M, Moreau P, Charbonnel C, Garban F, Hulin C, et al. Genetic abnormalities and survival in multiple myeloma: the experience of the intergroupe francophone du myelome. Blood 2007;109:3489–95.
34. Chong LC, Ben-Neriah S, Slack GW, Freeman C, Ennishi D, Mottok A, et al. High-resolution architecture and partner genes of MYC rearrangements in lymphoma with DLBCL morphology. Blood Adv 2018;2:2755–65.
35. King RL, McPhail ED, Meyer RG, Vasmatzis G, Pearce K, Smadbeck JB, et al. False-negative rates for MYC fluorescence in situ hybridization probes in B-cell neoplasms. Haematologica 2019;104:e248–e51.
36. May PC, Foot N, Dunn R, Geoghegan H, Neat MJ. Detection of cryptic and variant IGH-MYC rearrangements in high-grade non-Hodgkin's lymphoma by fluorescence in situ hybridization: implications for cytogenetic testing. Cancer Genet Cytogenet 2010;198:71–5.
37. Munoz-Marmol AM, Sanz C, Tapia G, Marginet R, Ariza A, Mate JL. MYC status determination in aggressive B-cell lymphoma: the impact of FISH probe selection. Histopathology 2013;63:418–24.
38. Peterson JF, Pitel BA, Smoley SA, Vasmatzis G, Smadbeck JB, Greipp PT, et al. Elucidating a false-negative MYC break-apart fluorescence in situ hybridization probe study by next-generation sequencing in a patient with high-grade B-cell lymphoma with IGH/MYC and IGH/BCL2 rearrangements. Cold Spring Harb Mol Case Stud 2019;5:a004077.
39. Szabo AG, Gang AO, Pedersen MO, Poulsen TS, Klausen TW, Norgaard P. Overexpression of c-myc is associated with adverse clinical features and worse overall survival in multiple myeloma. Leuk Lymphoma 2016;57:2526–34.
40. Moller HEH, Preiss BS, Pedersen P, Ostergaard B, Frederiksen M, Abildgaard N, et al. Myc protein overexpression is a feature of progression and adverse prognosis in multiple myeloma. Eur J Haematol 2018 July 12 [Epub ahead of print].
41. Duyao MP, Buckler AJ, Sonenshein GE. Interaction of an NF-kappa B-like factor with a site upstream of the c-myc promoter. Proc Natl Acad Sci U S A 1990;87: 4727–31.
42. Szalat R, Avet-Loiseau H, Munshi NC. Gene expression profiles in myeloma: ready for the real world? Clin Cancer Res 2016;22:5434–42.
43. Nguyen L, Papenhausen P, Shao H. The role of c-MYC in B-cell lymphomas: diagnostic and molecular aspects. Genes 2017;8:116.